Hydrotalcite/SBA15 composites for pre-combustion CO$_2$ capture: CO$_2$ adsorption characteristics

Jiaxi Peng[a, 1]

Diana Iruretagoyena[b, 1]

David Chadwick[b, *]

d.chadwick@imperial.ac.uk

[a]Department of Polymer Materials and Chemical Engineering, East China Jiaotong University, Nanchang, 330013, PR China

[b]Department of Chemical Engineering, Imperial College London, South Kensington, London, SW7 2AZ, UK

[*]Corresponding author.

[1]These co-authors contributed equally to the work.

Abstract

Hydrotalcite-like compounds (HT) show potential as CO$_2$ adsorbent materials for pre-combustion CO$_2$ capture applications, but require improvements in stability, adsorption capacity and kinetics. In this study, HT/SBA15 hybrids (with different Mg/Al ratios varying from 0.3 to 3) have been synthesised using a two-stage grafting method to coat a mesoporous SBA15 with hydrotalcite layers. The HT/SBA15 hybrids showed significant improvement in intrinsic CO$_2$ uptake (per mass of HT), initial uptake rate, and multicycle stability compared to unsupported HT. Compared to previously reported nanostructured carbon supports (e.g. CNF, MWCNTs), the HT/SBA15 hybrids were found to be more thermally stable and exhibit comparable adsorption uptake and rates. In particular, the use of SBA15 as a support is shown to prevent the gradual loss in weight from thermal decomposition observed for HT/MWCNT or HT/GO composites over extended cycling.

Keywords: CO$_2$; Adsorption; Hydrotalcite; SBA-15

1 Introduction

Over the last decades there has been widespread concern about the increasing concentration of carbon dioxide in the atmosphere due to anthropogenic activities, with fossil fuel combustion being the main CO$_2$ source [1]. There is, therefore, strong motivation in developing suitable processes for carbon dioxide capture and storage (CCS). Among a range of technologies suggested for this purpose, gas-solid adsorption appears as one of the most promising strategies for CO$_2$ capture applications. Unlike liquid sorbents, solid adsorbents can be used over a wide temperature range. Pre-combustion carbon capture is an attractive approach to CCS in which a developing technology is sorption-enhanced H$_2$ production, which operates between 573 and 773 K [2–4]. Numerous studies have proposed the use of hydrotalcite-like compounds for application as adsorbent materials in sorption-enhanced H$_2$ production [2–4].

Hydrotalcite-like compounds (HTs), also known as mixed-metal layered hydroxides or layered double hydroxides (LDHs), belong to a large class of anionic and basic clays. Their structure is composed of brucite Mg(OH)$_2$ layers, where Mg^{2+} is octahedrally coordinated by hydroxyl groups. These octahedra share adjacent edges to form sheets or layers. In HTs, some of the Mg^{2+} ions are replaced by Al^{3+} resulting in positive layers that are balanced by charge-compensating anions (e.g. Cl$^-$, CO$_3^{2-}$, SO$_4^{2-}$) located in the interlayer region, where hydrating water molecules are also accommodated. The general formula of HTs is: $\left(M_{1-x}^{2+}M_x^{3+}(OH)_2\right)^{x+}\left(A_{x/m}^{m-}\cdot nH_2O\right)^{x-}$ where M^{2+}, M^{3+} and A^{m-} commonly represent Mg^{2+}, Al^{3+} and CO$_3^{2-}$ respectively. Compared to other adsorbents, HTs are competitive at temperatures between ~473 K and ~723 K, exhibiting fast adsorption-desorption kinetics and being positively influenced by the presence of water [2,5]. In addition, they require less energy to be regenerated and show better stability upon cycling than other potential CO$_2$ adsorbents (e.g. calcium oxides) [3]. However, a major drawback of HTs for commercial use is their relatively low CO$_2$ adsorption capacities. In order to alleviate this weakness and to improve their overall adsorption performance, many studies have focused on modifying the chemistry of HTs by exchanging their structural ions and/or by incorporating alkali dopants [4,6–8]. It has also been reported that the CO$_2$ performance of HTs can be improved by supporting them with forms of carbon such as nanofibers (CNF) [6], multi-walled nanotubes (MWCNT) [9] and graphene oxide (GO) [10–12]. Although significant enhancement in terms of intrinsic capacity and regenerability have been achieved by the use of these carbon materials, thermal degradation of the support was observed over extended multicycles [10–12]. Composite mixtures of hydrotalcite with a more thermally stable material such as alpha alumina did not result in as marked enhancement of the activity or the stability as the observed with the nanostructured carbon supports [10,11].

Mesoporous silicas have been widely investigated as support materials in CO$_2$ sorption applications due to their pore structure, high surface area and hydrothermal stability. They have been functionalised with amines/polyetheneimine for low temperature CO$_2$

adsorption [13–18] and used as support for high temperature CO_2 adsorption by CaO-based sorbents [19]. Recently, Pramod et al. [20] investigated the CO_2 adsorption performance of HT-SBA15 composites at low temperature (343 K). Composites with Mg/Al ratio = 2 and a range of HT contents up to 50% were prepared by co-precipitation in an aqueous suspension of SBA-15. The HT/SBA15 adsorbents showed enhanced adsorption capacities and adsorption kinetics over pure hydrotalcite, Multicycle stability was also demonstrated over five cycles of adsorption at 343 K and desorption at 413 K. Very recently, Yilmaz [21] assessed the CO_2 adsorption performance of an amine modified hollow mesoporous silica-Mg-Al HT composite which showed high CO_2 uptake at 348 K and was found to be stable over four adsorption-desorption cycles. These studies demonstrate the utility of mesoporous silicas, and SBA-15 in particular, as support material for HT in CO_2 adsorption processes. However, the adsorption temperatures have been much lower than would be used in pre-combustion CCS or in the sorption enhanced water gas shift reaction (SEWGS).

In this paper we report the synthesis of HT/SBA15 hybrids with different Mg/Al ratios and their CO_2 adsorption performance tested at the higher adsorption temperature relevant for pre-combustion CCS applications (573 K) in contrast to earlier work on this type of material. The present HT/SBA15 composites were prepared free from residual sodium following a methodology adapted from the grafting approach reported recently by Creasey et al. [22]. The two step preparation method allows easy adjustment of the Mg/Al ratio while keeping the Al constant, and in principle, should favour porosity and mass transport involving the underlying silica architecture. We show that the SBA15 support confers significant advantage in terms of enhanced intrinsic adsorption capacity and adsorption kinetics compared to unsupported HT and previously reported HT-MWCNTs adsorbents [9]. The composites have also been tested over extended adsorption-desorption cycles and show good relative thermal stability and exhibit no gradual loss in weight which is a feature of HT on carbon nanostructure supports.

2 Experimental section

2.1 Materials

A mesoporous SBA15 was purchased from ACS Chemicals Supplier; aluminium-tn-sec-butoxide, triethylamine, magnesium methoxide solution, methanol, toluene, ethanol, $Mg(NO_3)_2 \cdot 6H_2O$ (99%), $Al(NO_3)_3 \cdot 9H_2O$ (98%), NaOH and Na_2CO_3 were purchased from Sigma-Aldrich.

2.2 Alumina grafting onto SBA15 (Al-SBA15)

The Al-SBA15 framework was synthesised following a methodology adapted from Creasey et al. [22] Triethylamine (0.525 mL) and SBA15 (0.25 g dried at 373 K), were added to a solution of 0.59 M Aluminum-tri-sec-butoxide in toluene. The resulting suspension was heated at 358 K for 6 h under stirring (300 rpm). The resulting suspension was filtered under vacuum using 0.4 μm polycarbonate membranes and washed three times with 25 mL of toluene at 333 K. The alumina surface was then hydrolysed in a mixture of ethanol (79.5 mL) and water (0.4 mL) for 24 h at 298 K under stirring. The solid was filtered using 0.4 μm polycarbonate membranes and washed with 75 mL of ethanol. The sample was dried for 12 h at 353 K. To produce an alumina monolayer in the sample, a three-step calcination sequence was used: The material was first heated to 523 K for 1 h, then 673 K for 1 h and finally 773 K for 4 h (at 1 K min^{-1}). Four consecutive grafting cycles were carried out using the same procedure (using 1 g of Al-SBA15 solid produced in the previous cycle).

2.3 Synthesis of hydrotalcite-coated SBA15 (HT-SBA15)

The as-synthesized Al-SBA15 sample (100 mg) was dried for 1 h at 353 K and then promoted by incipient wetness impregnation with a magnesium methoxide solution (8–10 wt% in CH_3OH). The sample was then stirred for 15 min and dried at 353 K for 1 h to remove the excess methanol. The volume of magnesium methoxide was varied to produce samples with different Mg:Al atomic ratios. 2.7 mL were used for the sample with a Mg:Al ratio 1:1. Subsequently, the sample was calcined at 723 K at 1 K min^{-1} for 15 h under 20 mL min^{-1} O_2. The sample was then cooled down to 298 K flowing 20 mL min^{-1} N_2. For every 75 mg powder, 12.5 mL of distilled water was added. The sample was then heated to 398 K and stirred overnight. Then, it was cooled down to room temperature, filtered, washed with 500 mL of water and dried in an oven for 24 h at 353 K. Four different HT-SBA15 hybrids were prepared with nominal Mg:Al ratios 0.3/1 (HT-SBA15-0.3), 1/1 (HT-SBA15-1), 2/1 (HT-SBA15-2) and 3/1 (HT-SBA15-3). A conventional hydrotalcite (HT) reference material with a Mg:Al ratio 2:1 was prepared via a coprecipitation technique (details are given elsewhere) [10].

2.4 Characterisation

The specific surface area and pore structure of the samples was determined by Brunauer-Emmett-Teller (BET), in which N_2 adsorption isotherms were measured at 77 K using a Tristar 3000 volumetric system. The samples were degassed at 393 K overnight under nitrogen. The phase composition of the samples was analysed by X-ray diffraction using a X'celerator detector (X'Pert PRO model), with a radiation source of Cu-Kα, a set voltage of 40 kV and set current of 20 mA. The morphology of the samples was investigated by STEM-EDS using a JEM-2100F instrument and Transmission electron microscopy using a JEOL 2000FX microscope. Thermogravimetric analysis (TGA), was performed in a TG209 F1 Libra NETZSCH coupled with mass spectroscopy. The sample (20 mg) was heated from 393 to 720 K at a heating rate of 10 K min^{-1} in 60 ml min^{-1} air. The elemental composition of the samples was determined by inductively coupled plasma-optical emission spectroscopy (ICP-OES) in a PerkinElmer Optima 2000DV instrument, and by energy dispersive spectroscopy (EDS) using an Oxford Instruments INCA energy dispersive X-ray spectrometer.

2.5 CO_2 adsorption measurements

The adsorption capacity, multicycle stability and kinetics of the samples were determined in a thermogravimetric analyser (PerkinElmer, TGA4000). The amount of adsorbent used in the CO_2-TGA experiments was relatively small varying from 5 to 20 mg and the samples were very fine particles in all cases. After the samples were pre-treated in situ by flowing 20 mL min^{-1} of N_2 at 673 K for 4 h, they were cooled down to 573 K and held for 10 min. The feed was then switched to a 20% CO_2/Ar premixed gas and held typically for 1 h. The adsorption capacity of the solid was determined from the change in mass during the CO_2 flow. The regeneration and stability of the samples was assessed by multicycle tests in which the adsorption step was carried out at 673 K during 30 min flowing nitrogen. In both steps the flow rate was kept at 20 mL min^{-1} during the experiment.

3 Results and discussion

3.1 Characterisation of the adsorbents

3.1.1 Chemical composition

The composition of the as-synthesised HT-SBA15 hybrids and the conventional unsupported HT are given in Table 1. The Mg/Al ratios of the adsorbents determined by ICP are close to the intended nominal ratios. Only traces of alkali impurities (Na and K) were detected in the materials at levels that are not expected to influence the CO_2 adsorption capacities. The Al/Si atomic ratio of the supported material was determined by EDS chemical analysis carried out over many representative sample regions. The ratios were found to be similar for all the HT-SBA15 samples, Table 1, and correspond to hydrotalcite loadings of ca. 25 wt.%. For the sample HT-SBA15-0.3, STEM-EDS mapping showed Al-rich and Si-rich regions originated from very poor dispersion; Mg could not be detected (i.e. below the detection limit), Fig. 1. Conversely, for higher Mg/Al ratios, the elements are well distributed in the samples indicating that a phase in which Mg and Al are in intimate contact (as expected for a layered double hydroxide) is effectively distributed over the SiO_2 support.

Table 1 Nominal and actual Mg/Al ratio, Al/Si ratio and XRD crystallite size of the as-synthesised adsorbents.

alt-text: Table 1

Sample name[a] As-synthesised adsorbents	Mg/Al (mol/mol) (nom.)	Mg/Al[b] (mol/mol) (actual)	Al/Si[c] (mol/mol)	XRD crystallite Size (nm)[d]
HT-SBA15-0.3	0.3/1	0.4/1	0.12	5
HT-SBA15-1	1/1	1.2/1	0.09	10
HT-SBA15-2	2/1	2.2/1	0.11	9
HT-SBA15-3	3/1	3.2/1	0.10	9
HT	2/1	2.2/1	—	13
SBA15				

[a] HT-SBA15-x, where x is the Mg/Al ratio of the sample.

[b] Determined by ICP.

[c] Determined by EDS.

[d] Calculated using the Scherrer equation.
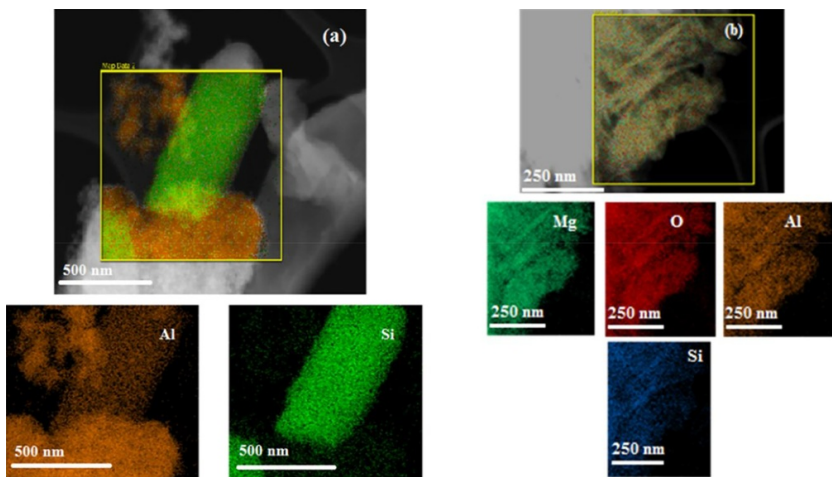
Fig. 1 STEM-EDS images of (a) HT-SBA15-0.3 and (b) HT-SBA15-2.

alt-text: Fig. 1

3.1.2 Transmission- ~~Electron and Scanning Electron M~~ *electron and scanning electron m*icroscopy

TEM micrographs show flake-shaped SBA15 crystallites with an average size of ~200 nm and a unidimensional mesopore structure with pore diameters of ca. 8.7 nm. In the case of HT-SBA15-0.3, an amorphous material is observed on top of the SBA15 particles which is likely to consist of excess aluminium from the grafting process. In contrast, for HT-SBA15-1, HT-SBA15-2 and HT-SBA15-3 the characteristic platelets of hydrotalcites are observed with approximately 40 nm and 10 nm in the lateral and through-thickness directions, respectively. Representative TEM images are shown in Figs. 2 and S1. The TEM images evidence that a significant part of the HT loading remains as crystallites supported on the SBA15 particles rather than as coating in the mesostructured channels. Remarkably, no isolated HT platelets were found in the TEM images; all appeared associated with SBA15 though often present as clusters of several HT platelets, particularly at high Mg loadings. SEM images of the dried HT-SBA15 hybrids show a porous, agglomerated powder, with a uniform dispersion of SBA15. As expected, an increase in the number of HT particles was observed with increasing the Mg/Al ratio content but no other morphological differences were apparent, Fig. 3.
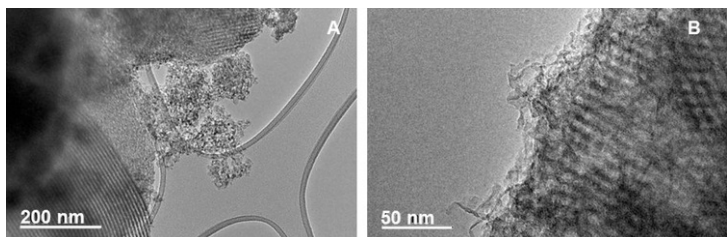

Fig. 2 Representative TEM images of HT-SBA15-0.3 and HT-SBA15-2.
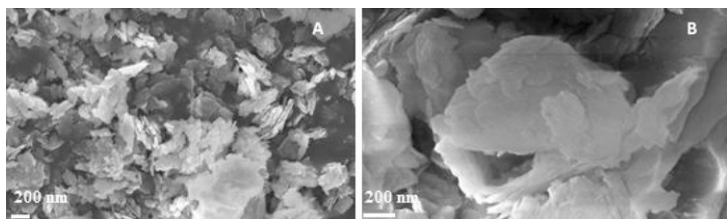
alt-text: Fig. 2

Fig. 3 Representative SEM images of HT-SBA15-0.3 and HT-SBA15-2.

3.1.3 Crystallographic characterisation

Powder X-ray diffraction patterns for the conventional HT and HT-SBA15 hybrids are shown in Fig. 4. The pure HT sample displays the reflections corresponding to two-dimensional hydrotalcite-like materials with carbonates in the interlayer (JCPDS no. 14-191) and can be indexed accordingly. The sample with Mg/Al ratio of 0.3 (HT-SBA15-0.3) exhibits broad diffraction peaks that correspond to the (003) and (006) planes of HT-like compounds together with reflections ascribed to an aluminium oxide hydroxide phase (boehmite). Increasing the Mg/Al ratio to 1 (HT-SBA15-1) increases the intensity of the HT features indicating that a larger part of the aluminium loading is incorporated into a double layer structure. Small peaks for the (020) and (021) planes of boehmite are still observable in this sample. The samples with higher Mg loadings (HT-SBA15-2 and HT-SBA15-3) exhibit the characteristic reflections of hydrotalcite. Small peaks of $Mg(OH)_2$ are visible in HT-SBA15-3 which has the highest Mg content. There is a clear shift in the position of the (003) and (006) reflections of HT for the HT-SBA15 hybrids towards higher 2θ values with increasing Mg content which stems from increased interlayer distances and unit cell parameters as more divalent cations are incorporated into the structure. The apparent size or coherence length in the c-direction (layer-stacking direction), as calculated by the Scherrer equation, increases from 5 nm in the Mg/Al = 0.3 sample to 9 nm in the Mg/Al = 3.0 sample, Table 1. The HT crystallite sizes of the hybrids with Mg/Al ratios between 1 and 3 are comparable to that of the conventional 2:1 hydrotalcite prepared by co-precipitation. Since the average HT crystallite size of the HT-SBA15 hybrids is of the order of magnitude of the mesopore diameters of the SBA15, it is apparent that only a minor part of the HT phase is coating the SBA15 channels, which is consistent with the TEM images, Fig. 2.
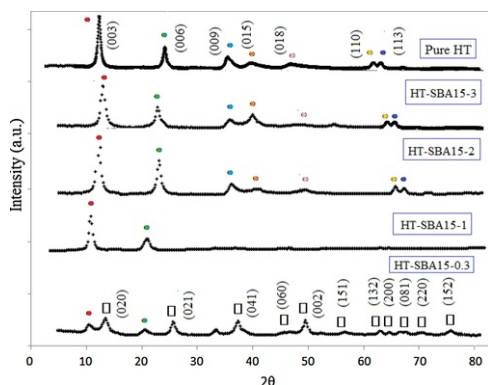

Fig. 4 XRD diffraction patterns of as-synthesised adsorbents. Characteristic reflections of HT (•), (□) Boehmite (AlO(OH)) and Mg(OH) (○).

After calcination at 673 K, the resulting HT hybrids lose the XRD features of the layered HT structure. Mainly weak, broad peak reflections at 37, 43 and 62 were observed, which correspond to diffraction by the (111), (200) and (220) planes of periclase (MgO, JCPDS No. 45-946); the aluminium is thought to be well-dispersed, (see Fig. S2 in the Supporting information).

3.1.4 Morphological characterisation

All the as-synthesised and activated materials exhibited type IV isotherms, see Figs. 5 and S3 respectively. The pure SBA15 presents some adsorption at low relative pressures that is ascribed to the micropores that interconnect the well-defined mesopore system. A narrow type H1 hysteresis loop is observed due to capillary condensation inside the cylindrical channels of uniform size. The isotherm of HT-SBA15-0.3 is very similar to that of the pure SBA15 although the uptake in the micropore region is reduced and the hysteresis is slightly broader. As the Mg/Al ratio increases, the isotherms resemble more the profile of the unsupported hydrotalcite: the micropore uptake decreases further and the narrow hysteresis loop extends over a wider range of reduced pressures (type H3). Type H3 hystereses are characteristic of plate-shaped particles forming non-uniform void slits as those prevailing within agglomerates of HT platelets. Creasey et al. [22] introduced macropores in the HT/SBA15 hybrids to aid the conversion of glyceryl triolein to FAME which are relatively large molecules. However, in this work, no macropores were introduced since they are not expected to offer an advantage in CO_2 uptake. The pure SBA15 sample shows a high surface area of 709 m^2/g and a pore volume of 1.4 cm^3/g. The average pore diameter of SBA15 determined by N_2 physisorption (7 nm) is reasonably close to the mesopore size determined from the TEM images. The corresponding pore size distributions of the as-synthesised materials are given in the Supporting information (Fig. S4). The surface area and pore volume of the HT-SBA15 hybrids decreases with increasing content of Mg in the hybrid, probably due to a combination of pore coating and blockage of the pore mouths by bigger HT platelets attached to the SBA15 particles, Table 2. As expected, the samples HT-SBA15-2 and HT-SBA15-3, containing Mg/Al ratios of 2 and 3 respectively, show surface areas comparable to that of the conventional HT sample, suggesting that the pores of the SBA15 are mainly saturated with HT. This is in agreement with the results reported by Pradmod et al. [20] who observed a fall in the average pore volume of HT/SBA15 hybrids containing more than 20% wt. HT due to pore saturation. For the unsupported HT and the samples containing a 3:1 and 2:1 Mg/Al ratios, the surface area increases upon calcination whereas for the pure SBA15 and the samples with low Mg/Al ratios remains practically constant.
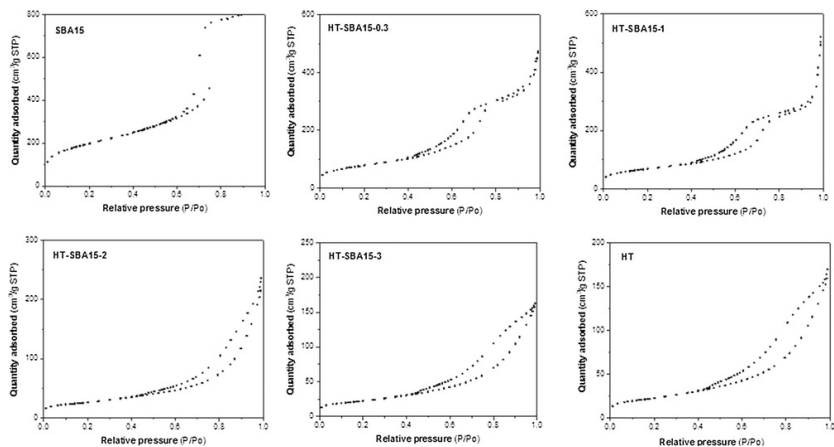
Fig. 5 N_2 physisorption isotherms of as-synthesised adsorbents

alt-text: Fig. 5

Table 2 Physicochemical properties of the as-synthesized and activated adsorbents.

alt-text: Table 2

Sample name[a]	As-synthesised adsorbents			Sample name	Activated adsorbents		
	S_{BET} (m²/g)	Vpore (cm³/g)	Pore size (nm)		~~Sample name~~S_{BET} (m²/g)	Vpore (cm³/g)	Pore size (nm)
HT-SBA15-0.3	496	1.10	6.2	HT-SBA15-0.3_act	489	1.30	5.9
HT-SBA15-1	242	0.50	6.2	HT-SBA15-1_act	239	0.40	7.0
HT-SBA15-2	79	0.30	7.8	HT-SBA15-2_act	123	0.15	4.0
HT-SBA15-3	77	0.40	7.5	HT-SBA15-3_act	118	0.17	5.0
HT	95	0.30	8.0	HT_act	150	0.50	7.0
SBA15	709	1.40	7.0	SBA15_act	709	1.39	7.0

a HT-SBA15-x, where x is the Mg/Al ratio of the sample.

3.1.5 Thermal gravimetric analysis

The TGA patterns of SBA15, the unsupported HT, and the HT-SBA15 hybrids are shown in Fig. 6a. The pure SBA15 presents a broad water desorption peak that extends from 400 to 720 K and corresponds to less than 2.5% of weight loss. On the other hand, the pure unsupported hydrotalcite loses ca. 35% of its weight over three distinctive stages that correspond to dehydroxylation (below ~483 K), partial dehydroxylation and decarbonation (between ~483 K and ~720 K), and further decarbonation (above ~720 K). For the HT-SBA15 hybrids the weight loss increases with the magnesium content but occurs in the same three stages observed for the unsupported HT. A remarkable feature is that, for the same Mg/Al ratio, the partial dehydroxilation/decarbonation and the final decarbonation peaks shift towards higher temperatures (ca. 20–30 K) in the HT-SBA15 hybrid compared to the unsupported hydrotalcite, Fig. 6b. This is attributed to an increased probability of re-adsorption of water and CO_2.
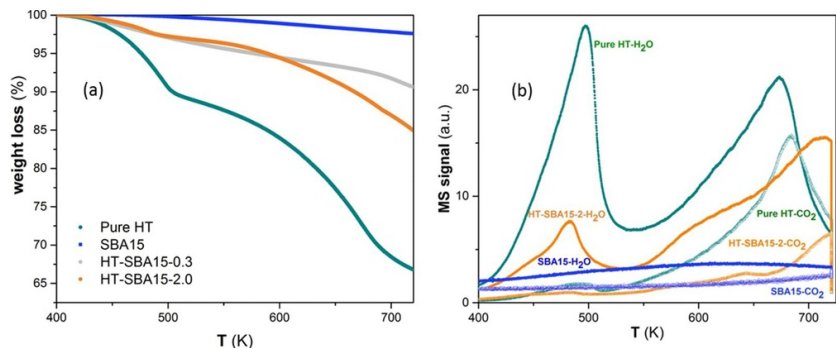
Fig. 6 (a)Thermograms of Pure HT, SBA15, HT-SBA15-0.3 and HT-SBA15-2 hybrids (b) Evolution of CO_2 and H_2O species.

alt-text: Fig. 6

3.2 CO_2 adsorption capacity measurements

The CO_2 adsorption capacity of the materials during the first exposure to the adsorptive gas (P CO_2 = 200 mbar) was measured at 573 K and corresponds to the average of at least five separate measurements, Table 3. The CO_2 uptake of pure SBA15 is negligible under the conditions of the experiments. The adsorption capacity of the unsupported HT showed good reproducibility among the set of tests performed (standard deviation of 0.02). On the other hand, the HT-SBA15 hybrids exhibited variable adsorption capacities with standard deviations around 0.1. This result was attributed to heterogeneity in the material on the scale of mass used for TGA (20 mg). However, there is a clear trend showing that the mean adsorption capacities under dry conditions increase with the Mg content. Indeed, there is a remarkable improvement in the CO_2 uptake per mass of HT (i.e. intrinsic capacity) for the HT-SBA15-1, HT-SBA15-2 and HT-SBA15-3 compared to the unsupported HT sample, Table 3 with the enhancement increasing with the Mg:Al ratio and the conversion of the Al layer to hydrotalcite. This is consistent with the X-ray diffractograms that show better defined layered structures with increasing Mg content resulting in more intimate contact between Mg and Al in the mixed oxides obtained after thermal activation. Previous studies have shown that hydrotalcites with Mg:Al ratio 2:1 and 3:1 exhibit optimal performance for CO_2 adsorption [23,24].

Table 3 First-contact adsorption capacities and adsorption rates of the adsorbents at 573 K and PCO_2 = 200 mbar.

alt-text: Table 3

Sample[a]	wt% support	Mg/Al (nom)	First-contact capacities (mol CO2/- CO_2/kg HT)	First contact capacities (mol CO_2/-kg ads)	Adsorption rate (mol CO_2/-kg HT min)
HT_act	0	2/1	0.30	0.30	0.22
HT-SBA15-0.3_act	75	0.3/1	0.20	0.05	0.01
HT-SBA15-1_act	75	1/1	0.51	0.13	0.18
HT-SBA15-2_act	75	2/1	0.56	0.14	0.30
HT-SBA15-3_act	75	3/1	0.75	0.19	0.35

[a] HT/SBA-15-x where x is the Mg/Al ratio.

The adsorption capacities of the HT-SBA-15 composites are compared with previous values for HT-SBA15 reported by Pramod et al. [20], carbon composites of similar HT loadings (HT/CNF and HT/MWCNTs), a commercial HT/Al$_2$O$_3$, and HT/GO in Table 4. The present HT-SBA15 composites showed lower adsorption capacities than those reported by Pramod et al. [20]. However, these measurements are not directly comparable with the present work since the CO_2 adsorption was carried out at much lower adsorption temperature (which increases strongly the adsorption). After correcting for the temperature difference, the intrinsic adsorption capacities of the co-precipitated HT-SBA15 composites appear higher than the present HT-SBA15. However, the materials are not strictly comparable since the hydrotalcite composites prepared by Pramod et al. [20] were calcined at a significantly lower temperature (473 K) than the present study (673 K), leading to incomplete activation to mixed oxides. The intrinsic capacity and capacity per total mass of adsorbent of HT-SBA15-3 are either similar or higher than values for carbon or alumina supported HT, Table 4, in part due to the higher Mg content, confirming the attraction of SBA-15 as a support material. As expected, HT/GO shows lower intrinsic capacity than HT-SBA15-3, but higher capacity per mass of adsorbent since the content of GO is only 20 wt%.

Table 4 First-contact adsorption capacities of the adsorbents.

alt-text: Table 4

Authors	Samples[a]	Temp. (K)	wt% support	Mg/Al (nom)	First-contact capacities (molCO_2/-kg HT)	First contact capacities (mol CO_2/-kg ads)	Adsorption rate (mol CO_2/kg HT min)
Ref. [6]	HT/CNF_act	523	90	2/1	1.30 (1.1)[b]	0.13	–
Ref. [10]	HT/GO_act	573	20	2/1	0.30	0.24	–
Ref. [9]	HT/Al$_2$O$_3$_act	573	80	2/1	0.43	0.09	–
Ref. [9]	HT/MWCNTs_act	573	67	2/1	0.58	0.19	0.26
Ref. [20]	HT/SBA15_act	343	50	2/1	7.20 (1.8)[b]	3.60	–
Present work	HT-SBA15-3_act	573	75	3/1	0.75	0.19	0.35

Ref. [6] (activated at 773 K, wet CO_2, PCO_2 = 50 mbar)

   Ref. [9] (activated at 673 K, dry CO_2, 573 K, PCO_2 = 200 mbar)

   Ref. [10] (activated at 673 K, dry CO_2, 573 K, PCO_2 = 200 mbar)

   Ref. [20] (activated at 473 K, dry CO_2, 343 K, PCO_2 = 100 mbar).

   Present work (activated at 673 K, dry CO_2, 573 K, PCO_2 = 200 mbar).

[a] HT-SBA15-x, where x is the Mg/Al ratio of the sample.

[b] Estimated adsorption capacities at 573 K. Values were obtained using the estimated heats of adsorption (3.7 kJ mol^{-1} , [6] and 1.1 kJ mol^{-1} [20]).

The initial adsorption rates for the unsupported HT, the HT-SBA15 and HT/MWCNT hybrids were calculated from the slope of the weight-gain curve at time zero. The influence of the film resistance on the adsorption experiments was assessed by changing the mass loaded on the TGA pan and/or the flow rate while keeping a constant granule size (100–350 μm). Regardless of the mass space velocity, the CO_2 adsorption capacities after 120 minutes of exposure were found to be the same (within the uncertainty of the apparatus) for a given sample, indicating that inter-particle transfer limitations are minimal. For the HT-SBA15 composites, the uptake rate per mass of HT increases with the Mg/Al ratio as shown in Table 3. For the sample with Mg/Al = 0.3 the low rate can be related to the poor layer structure before activation, as revealed by XRD. On the other hand, the initial adsorption rate per mole of Mg is comparable for the SBA15 hybrids with Mg/Al ratios 1:1, 2:1 and 3:1, indicating that for the fresh materials the accessibility to the adsorption sites is independent of the HT composition. The superior adsorption rates observed for the HT/SBA15 for high Mg/Al ratios, Tables 3 and 4, in part reflects the higher Mg content but could also be related to improved diffusion of CO_2 over the external surface of the SBA15.

3.2.1 Adsorption-desorption thermal cycling

Continuous adsorption-desorption cycles were carried out to assess the regeneration and stability of the adsorbents under dry conditions, Fig. 7. The CO_2 capacity of the pure HT and the HT-SBA15 hybrids drops markedly during the first cycle and becomes stable gradually. This indicates that during the first contact between the adsorbent and the adsorptive gas some CO_2 is irreversibly chemisorbed on the fresh material and then reversible adsorption dominates with parallel thermal sintering. Similar trends have been reported for studies dealing with adsorption of CO_2 on HT-containing adsorbents at relatively high temperatures [5,7,8].
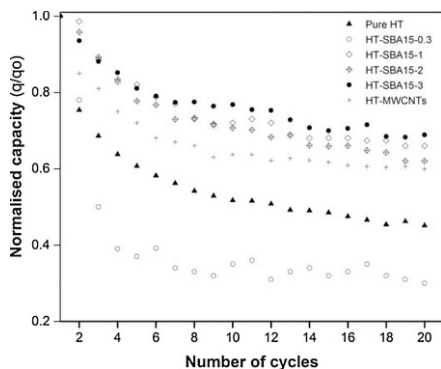
Fig. 7 Normalised CO$_2$ adsorption capacity over 20 adsorption-desorption cycles.

alt-text: Fig. 7

The presence of SBA15 in the hybrids HT-SBA15-1, HT-SBA15-2 and HT-SBA15-3 enhances considerably the stability of the pure HT sample, and was found to be independent of the Mg/Al ratio in the hybrid. Similar to the adsorption capacity, the stability of the HT-SBA15-0.3 hybrid was very poor probably due to its poor layer structure before activation, as revealed by XRD. The performances of the HT-SBA15 hybrids were compared with that of a HT-MWCNT sample. The stability of the MWCNT adsorbent was superior to that of unsupported HT. However, it was evident that the HT-SBA15 supported hybrids were markedly more stable than the HT-MWCNT hybrid, which is possibly attributed to the large pores and thick walls of the SBA15 making it very hydrothermally stable [25]. In previous studies, we have shown that although the multicycle stability of the CO$_2$ adsorption capacity of HT/MWCNTs and HT/GO is improved compared to the pure HT, both materials exhibit a gradual loss of weight over cycling probably due to the evolution of residual functional groups present in the MWCNTs and GO [9,12]. Remarkably, the HT/SBA15 hybrids do not lose weight significantly over extended cycling, which make them more attractive adsorbents for pre-combustion CCS or SEWGS applications, Fig. 8.
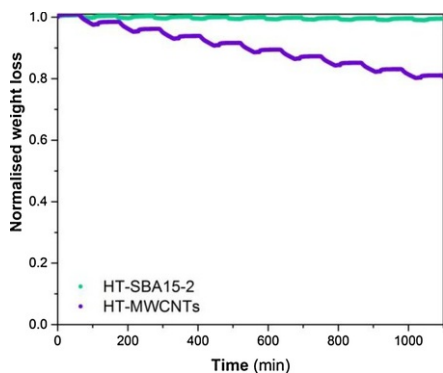

Fig. 8 Weight loss upon adsorption-desorption cycling (573 K adsorption and 673 K desorption, time equivalent to 11 adsorption-desorption cycles). HT/GO follows a trend similar to HT-MWCNTand is omitted for clarity.

alt-text: Fig. 8

4 Conclusions

The CO$_2$ adsorption performance of HT/SBA15 hybrids with different Mg/Al ratios have been tested at an adsorption temperature relevant for pre-combustion CCS applications (573 K). Remarkably, no isolated HT platelets were found in TEM images. This study shows that mesoporous SBA15 is an efficient support for HTs for CO$_2$ adsorption. The CO$_2$ adsorption capacity per mass of HT of the activated hybrids was found to increase when supported on SBA15 and it generally increased with the Mg/Al ratio. The higher intrinsic capacities for the supported samples stem from an improved accessibility of the adsorptive gas to the active sites when the HT is well dispersed over a high surface area support. The multicycle stability of the hydrotalcite was also significantly increased when supported on SBA15 but was found to be independent of the Mg/Al ratio. The initial adsorption rates for the unsupported HT was also improved by the addition of SBA15 particularly for high Mg/Al ratios possibly due to improved diffusion of CO$_2$ over the external surface of the SBA15 and enhanced CO$_2$ contact with HT layers. Compared to other HT supports (e.g. CNF, Al$_2$O$_3$, MWCNTs and GO), SBA15 hybrids were found to be generally more thermally stable and exhibit slightly higher adsorption uptake and rates. The use of SBA15 as support was found to prevent the gradual weight loss over thermal cycling observed with the other supports. The two-step grapfting approach used here lends itself to the synthesis of materials containing macropores as reported by Creasy et al. [22].

Acknowledgements

Appendix A. Supplementary data

Supplementary material related to this article can be found, in the online version, at doi:https://doi.org/10.1016/j.jcou.2017.12.004

References

[1] J.-R. Li, Y. Ma, M.C. McCarthy, J. Sculley, J. Yu, H.-K. Jeong, P.B. Balbuena and H.-C. Zhou, Carbon dioxide capture-related gas adsorption and separation in metal-organic frameworks, *Coordination Chemistry Reviews* *Chem. Rev.* **255** (15–16), 2011, 1791–1823.

[2] Y. Ding and E. Alpay, Equilibria and kinetics of CO2 adsorption on hydrotalcite adsorbent, *Chemical Engineering Science* *Eng. Sci.* **55** (17), 2000, 3461–3474.

[3] S. Choi, J.H. Drese and C.W. Jones, Adsorbent materials for carbon dioxide capture from large anthropogenic point sources, *ChemSusChem* **2** (9), 2009, 796–854.

[4] D. Iruretagoyena Ferrer, Introduction, Supported Layered Double Hydroxides as CO2 Adsorbents for Sorption-Enhanced H2 Production, 2016, Springer International Publishing; Cham, 1–6.

[5] Y. Ding and E. Alpay, High temperature recovery of CO2 from flue gases using hydrotalcite adsorbent, *Process Saf. Environ. Prot.* **79** (1), 2001, 45–51.

[6] N.N.A.H. Meis, J.H. Bitter and K.P. de Jong, Support and size effects of activated hydrotalcites for precombustion CO2 capture, *Ind. Eng. Chem. Res.* **48** (3), 2009, 1229–1235.

[7] N.D. Hutson and B.C. Attwood, High temperature adsorption of CO2 on various hydrotalcite-like compounds, *Adsorption* **14** (6), 2008, 781–789.

[8] D. Iruretagoyena, X. Huang, M.S.P. Shaffer and D. Chadwick, Influence of alkali metals (Na, K, and Cs) on CO2 adsorption by layered double oxides supported on graphene oxide, *Ind. Eng. Chem. Res.* **54** (46), 2015, 11610–11618.

[9] A. Garcia-Gallastegui, D. Iruretagoyena, M. Mokhtar, A.M. Asiri, S.N. Basahel, S.A. Al-Thabaiti, A.O. Alyoubi, D. Chadwick and M.S.P. Shaffer, Layered double hydroxides supported on multi-walled carbon nanotubes: preparation and CO2 adsorption characteristics, *J. Mater. Chem.* **22** (28), 2012, 13932.

[10] D. Iruretagoyena, M.S.P. Shaffer and D. Chadwick, Layered double oxides supported on graphene oxide for CO2 adsorption: effect of support and residual sodium, *Ind. Eng. Chem. Res.* **54** (26), 2015, 6781–6792.

[11] D. Iruretagoyena, M.S.P. Shaffer and D. Chadwick, Adsorption of carbon dioxide on graphene oxide supported layered double oxides, *Adsorption* **20** (2), 2014, 321–330.

[12] A. Garcia-Gallastegui, D. Iruretagoyena, V. Gouvea, M. Mokhtar, A.M. Asiri, S.N. Basahel, S.A. Al-Thabaiti, A.O. Alyoubi, D. Chadwick and M.S.P. Shaffer, Graphene oxide as support for layered double hydroxides: enhancing the CO2 adsorption capacity, *Chem. Mater.* **24** (23), 2012, 4531–4539.

[13] X. Xu, C. Song, J.M. Andrésen, B.G. Miller and A.W. Scaroni, Preparation and characterization of novel CO2 "molecular basket" adsorbents based on polymer-modified mesoporous molecular sieve MCM-41, *Microporous Mesoporous Mater.* **62** (1), 2003, 29–45.

[14] A. Sayari, Modified Adsorbent for Dry Scrubbing and Use Thereof, Google Patents (2006).

[15] R. Serna-Guerrero and A. Sayari, Modeling adsorption of CO2 on amine-functionalized mesoporous silica. 2: kinetics and breakthrough curves, *Chem. Eng. J.* **161** (1), 2010, 182–190.

[16] C.F. Martín, M.B. Sweatman, S. Brandani and X. Fan, Wet impregnation of a commercial low cost silica using DETA for a fast post-combustion CO2 capture process, *Appl. Energy* **183**, 2016, 1705–1721.

[17] L. Zhou, J. Fan, G. Cui, X. Shang, Q. Tang, J. Wang and M. Fan, Highly efficient and reversible CO2 adsorption by amine-grafted platelet SBA-15 with expanded pore diameters and short mesochannels, *Green Chem.* **16** (8), 2014, 4009–4016.

[18] X. Guo, L. Ding, K. Kanamori, K. Nakanishi and H. Yang, Functionalization of hierarchically porous silica monoliths with polyethyleneimine (PEI) for CO2 adsorption, *Microporous Mesoporous Mater.* **245**, 2017, 51–57.

[19] C.-H. Huang, K.-P. Chang, C.-T. Yu, P.-C. Chiang and C.-F. Wang, Development of high-temperature CO2 sorbents made of CaO-based mesoporous silica, *Chem. Eng. J.* **161** (1), 2010, 129–135.

[20] C.V. Pramod, K. Upendar, V. Mohan, D.S. Sarma, G.M. Dhar, P.S.S. Prasad, B.D. Raju and K.S.R. Rao, Hydrotalcite-SBA-15 composite material for efficient carbondioxide capture, *J. CO2 Util.* **12**, 2015, 109–115.

[21] M. Sari Yilmaz, Synthesis of novel amine modified hollow mesoporous silica@Mg-Al layered double hydroxide composite and its application in CO2 adsorption, *Microporous Mesoporous Mater.* **245**, 2017, 109–117.

[22] J.J. Creasey, C.M.A. Parlett, J.C. Manayil, M.A. Isaacs, K. Wilson and A.F. Lee, Facile route to conformal hydrotalcite coatings over complex architectures: a hierarchically ordered nanoporous base catalyst for FAME production, *Green Chem.* **17** (4), 2015, 2398–2405.

[23] J.-I. Yang and J.-N. Kim, Hydrotalcites for adsorption of CO2 at high temperature, *Korean J. Chem. Eng.* **23** (1), 2006, 77–80.

[24] Z. Yong and A.E. Rodrigues, Hydrotalcite-like compounds as adsorbents for carbon dioxide, *Energy Convers. Manage.* **43** (14), 2002, 1865–1876.

[25] A.K.O. Rodrigues, J.E.T. Ramos, C.L. Cavalcante Jr, E. Rodríguez-Castellón and D.C.S. Azevedo, Pd-loaded mesoporous silica as a robust adsorbent in adsorption/desorption desulfurization cycles, *Fuel* **126**, 2014, 96–103.

Appendix A. Supplementary data

The following ~~is~~ is Supplementary data to this article:

[Multimedia Component 1](#)

Graphical abstract
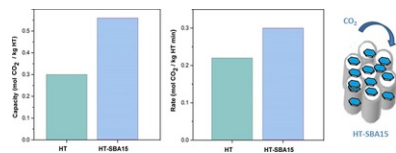
Highlights

- HT/SBA-15 with different Mg/Al prepared by two-stage grafting approach.

- HT/SBA15 has enhanced capacity, kinetics and stability compared to pure HT.

- Use of SBA15 prevents the gradual weight loss over cycling seen with nanostructured carbon supports.

Queries and Answers

Query: Please check the presentation for all the Tables and correct if necessary.
Answer:

Query: Your article is registered as a regular item and is being processed for inclusion in a regular issue of the journal. If this is NOT correct and your article belongs to a Special Issue/Collection please contact s.sankaran@elsevier.com immediately prior to returning your corrections.
Answer:

Query: The author names have been tagged as given names and surnames (surnames are highlighted in teal color). Please confirm if they have been identified correctly.
Answer:

Query: Please check the e-mail address for corresponding author and correct if necessary.
Answer:

Query: Please check whether the designated corresponding author is correct, and amend if necessary.
Answer:

Query: Please check the hierarchy of the section headings.
Answer:

Query: One or more sponsor names and the sponsor country identifier may have been edited to a standard format that enables better searching and identification of your article. Please check and correct if necessary.

Answer: